Geologie en Mijnbouw **73:** 415–424, 1994.

Seismic hazard assessment for the Lower Rhine Embayment before and after the 1992 Roermond earthquake

Werner Rosenhauer[1] & Ludwig Ahorner[2]
[1] *Siemens AG, Postfach 3220, D–91050 Erlangen,* [2]*Department of Earthquake Geology, Geological Institute, University of Cologne, Vinzenz-Pallotti-Str. 26, D-51429 Bergisch Gladbach, Germany*

Received 14 June 1993; accepted in revised form 8 December 1993

Key words: hazard map, Monte-Carlo simulation, occurrence frequency, statistics of extremes

Abstract

A regional probabilistic seismic hazard analysis for the Lower Rhine Embayment was published by the authors in 1975 and updated in 1984 as part of a comprehensive study for the former Federal Republic of Germany and adjacent regions. The seismic zones of the Lower Rhine Embayment were found to belong to the most active in western and central Europe. This contribution presents the modifications required after the occurrence of the Roermond earthquake of April 13, 1992.

New frequency–magnitude curves $\lambda(> M)$ are derived as the essential quantitative input, applying the generalized Gumbel distribution for magnitude extremes. Completion of the former data for the years 1980–1992 leads to distinct changes of $\lambda(> M)$ in the seismic zone in which the epicenter of the Roermond earthquake is situated.

Revised frequency–intensity curves $\lambda(> I)$ are computed with the Monte-Carlo simulation techniques using code PSSAEL developed earlier by the authors. Only small changes are found. For example, an intensity (MSK) I = VII is now expected at Roermond for future events with a probability of $4.9 \cdot 10^{-4}$/year instead of $2.4 \cdot 10^{-4}$/year.

The regional seismic risk is illustrated by two recomputed hazard maps of the Lower Rhine Embayment.

Introduction

The authors' first probabilistic seismic hazard analysis of the Lower Rhine Embayment was performed about twenty years ago (Ahorner & Rosenhauer 1975), and significant progress has been made since. This early study covers the essential features of the regional seismicity, but addressed peak acceleration and its distribution, a quantity which has not been considered to be the most suitable hazard parameter at western and central European sites thereafter. The much better known macroseismic intensity (MSK-scale) has been used as a more appropriate characterization of the site ground motion in all later analyses, although it is originally a risk parameter by definition, since it includes damage in addition to hazard. Intensities are nevertheless usually accepted as hazard data, for instance at uninhabited places when drawing isoseismal maps. Design spectra correlated to intensity have been available for many years (Hosser & Maurer 1986), establishing the intensity as the superior key parameter of the hazard assignment. The predominant reason for the use of intensity has been, among others, that its attenuation model and its correlation with Richter magnitudes could be based on local data (Ahorner 1983).

Satisfactory magnitude occurrence frequency curves $\lambda(>M)$ were derived since about 1978 by improved statistical evaluations of magnitude extremes applying the generalized Gumbel distribution (Rosenhauer 1983). Extremes are simply the largest values of a quantity in subsequent time intervals of equal length T, for example the N = 25 largest of the magnitudes determined or estimated for earthquakes in the seismic zone NRB 2 of the Lower Rhine Embayment in the years 1750–1759, 1760–1769 etc. with T = 10 years (cf. Fig. 4).

Extremes have been used in numerous investigations during the last decades, (e.g. Burton 1979, who also gives an extensive survey of earlier work). For periods in the past the extremes are less severely

afflicted with the incompleteness of information than the entire set of an unknown number of events. A more detailed description of the theory and its most important implications (Rosenhauer & Ahorner 1991) is briefly reviewed in this paper. Illustrative additional applications using two kinds of unbiased statistical plots are presented in the next section.

The Monte-Carlo code PSSAEL (Probabilistic Seismic Site Analysis using Earthquake Libraries) was ready for use since about 1980 and has been employed without major changes in many analyses. Besides having other advantages, it processes the magnitude dependence of the focal depths and, most important, manages a stochastic model of the intensity attenuation (Rosenhauer 1983, Ahorner & Rosenhauer 1993).

The authors' hazard investigations of the Lower Rhine Embayment were carried out as part of a more extensive study for the former Federal Republic of Germany and adjacent regions, comprising a total area of $48 \cdot 10^4$ km^2 (Hosser et al. 1983, Rosenhauer 1984, Ahorner & Rosenhauer 1986). Figure 1 shows a resulting probabilistic map of the seismic hazard, which was obtained from computations for a grid of more than 700 sites. Figure 2 shows the zones of the underlying seismicity model.

Extensive statistical evaluations of the ample extreme values of this total area permitted a reliable and accurate estimation of its upper magnitude bound. $M_{max} = 6^3/_4$ was adopted as a conservative value (Rosenhauer & Ahorner 1991, Ahorner & Rosenhauer 1993). This was used as a guideline for the deterministic choice of smaller values of M_{max} in the subzones, in which the extent of the data did not allow a statistically significant determination. As a general rule, M_{max} was taken at least 0.5 above the magnitude of the strongest observed event within the zone. Numerous analyses proved, however, that the influence of these upper bounds on the intensity-frequency curve $\lambda(> I)$ is negligible when using the generalized Gumbel distribution for the frequency–magnitude relations $\lambda(> M)$.

The seismic zones of the Lower Rhine Embayment, NRB 1 with an area of $0.76 \cdot 10^4$ km^2 and $M_{max} = 6^1/_4$ as well as NRB 2 with an area of $0.27 \cdot 10^4$ km^2 and $M_{max} = 6^3/_4$, were both judged capable of an event like the Roermond earthquake. This outstanding earthquake occurred in NRB 1. Including the Roermond earthquake of April 13, 1992 and other large events in zone NRB 1 and NRB 2, respectively, as extreme values for the years 1980–1992 improves the basic data and facilitates the derivation of occurrence frequencies $\lambda(> M)$ (next section). Figure 3 shows the revised seismic zonation near the Roermond earthquake, i.e. without changes of the border lines of the earlier zonation (Fig. 2), but with some additional zones in the former 'background' of extremely low seismicity.

Evaluation of extremes

The generalized Gumbel distribution implies a smooth shape of the frequency–magnitude curve $\lambda(> M)$ determined by three independent parameters $m = m(T)$, $\sigma = \sigma(T)$ and τ:

$$\lambda(> M) \cdot T = \left(f_1 - f_2 \frac{M - m(T)}{\sigma(T)} \right)^{1/\tau} \qquad (1)$$

where $f_1 = \Gamma(1 + \tau)$, $f_2 = \sqrt{\Gamma(1 + 2\tau) - f_1^{\,2}}$, Γ Gamma function, T reference time (for extremes) and $M < M_{max} = m(T) + \sigma(T)\, f_1/f_2$.

It provides a finite upper magnitude bound M_{max} for $\tau > 0$ (cf. Fig. 8) and is approaching a straight line in a logarithmic plot for $\tau = 0$ (Rosenhauer & Ahorner 1991). A value of $\tau > 0$ may therefore be interpreted as the curvature parameter of $\log \lambda(> M)$, characterizing the deviation from the wellknown Gutenberg and Richter law (limiting straight line, $\tau = 0$):

$$\log\lambda(> M) = a - b\, M \qquad (2)$$

The parameters $m = m(T)$ and $\sigma = \sigma(T)$ can be shown to be the mean value and the standard deviation of T-extremes, respectively, a fact supplying the usual statistical estimates from the first and the second empirical moment of observed extremes for these quantities. τ is connected with the third empirical moment via the distribution skewness (Rosenhauer 1983).

Figure 4 gives an example data set of ordered magnitude extremes for NRB 2. It explains how m and σ may alternatively be determined from a plotted straight line, in analogy to the well known probability graph paper for the normal distribution. This is supposing that the shape parameter $0 < \tau < 1$ was estimated before ($\tau = 0.33$ in the example) by a direct statistical evaluation of the observed extremes, for instance according to Rosenhauer (1983). Plots based on simple plotting positions like $x_i = i/(N + 1)$ would produce an unacceptable bias for a small total number N of extremes. Here, bias is avoided by a more careful analysis, taking the lowest value x_1, the second x_2 etc. which would be expected under the assumptions of equal τ, but with

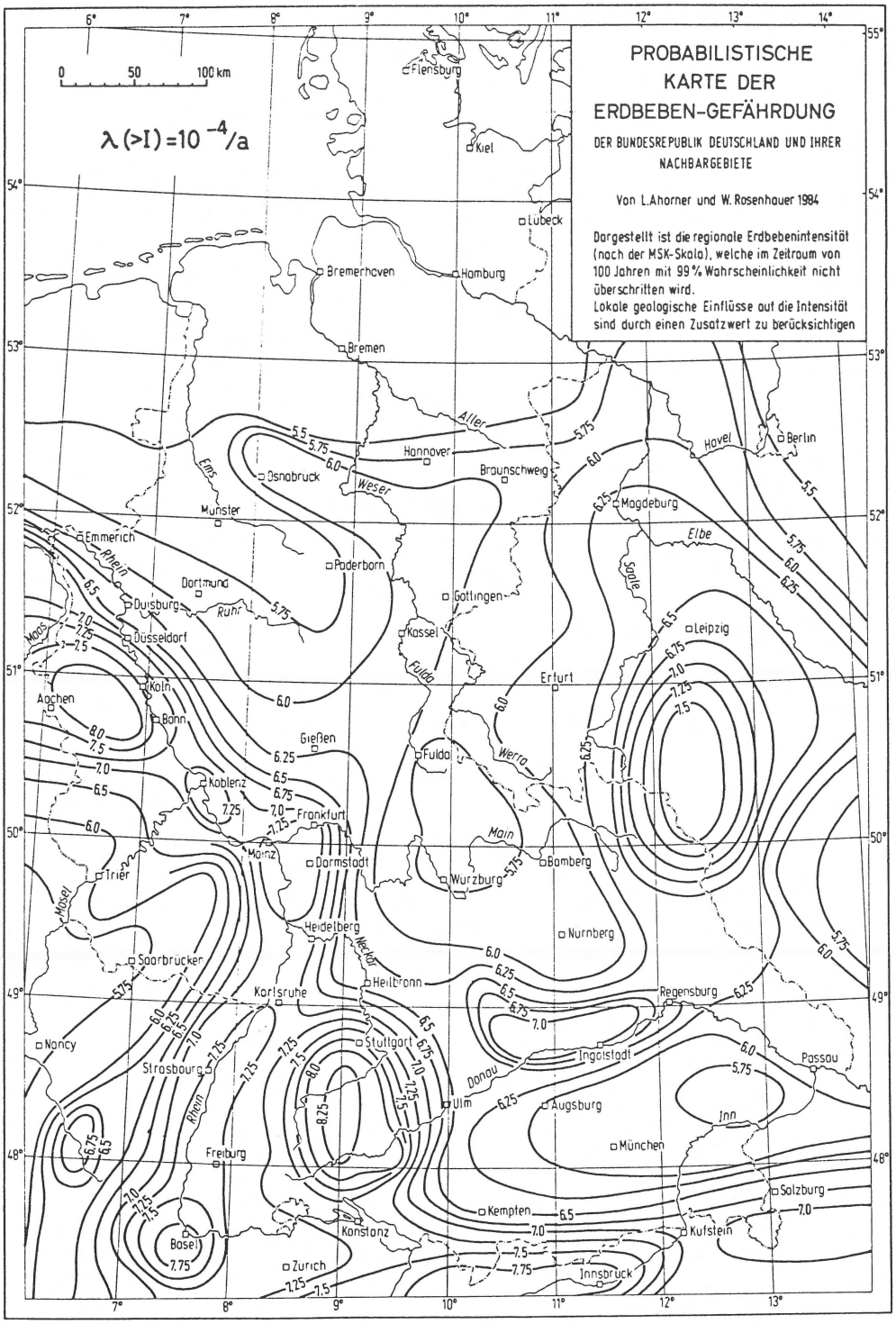

Fig. 1. Seismic hazard map of Germany and adjacent regions prepared by Ahorner & Rosenhauer in 1984 (see Ahorner & Rosenhauer 1986, 1993). Isolines give the regional macroseismic intensities (MSK) for an annual occurrence frequency $\lambda(>I) = 10^{-4}$. Local geological influences have to be taken into account by special site corrections.

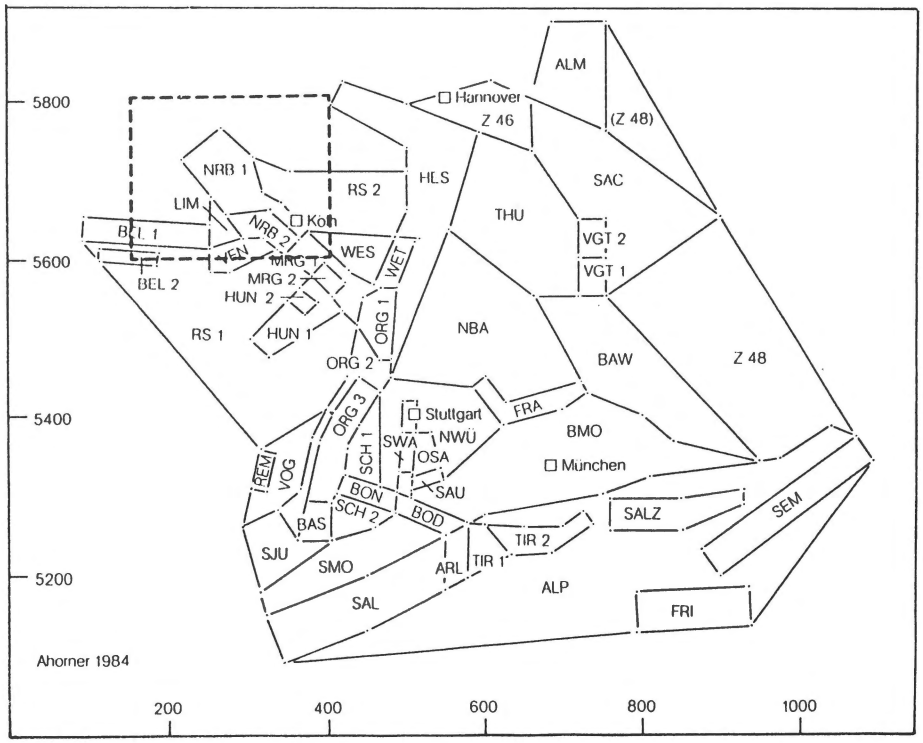

Fig. 2. Seismic zones underlying the 1984 hazard map (Fig. 1). Box (dashed lines) indicates area for which seismic hazard has been re-assessed (Fig. 3). Coordinates UTM Zone 32 U (km).

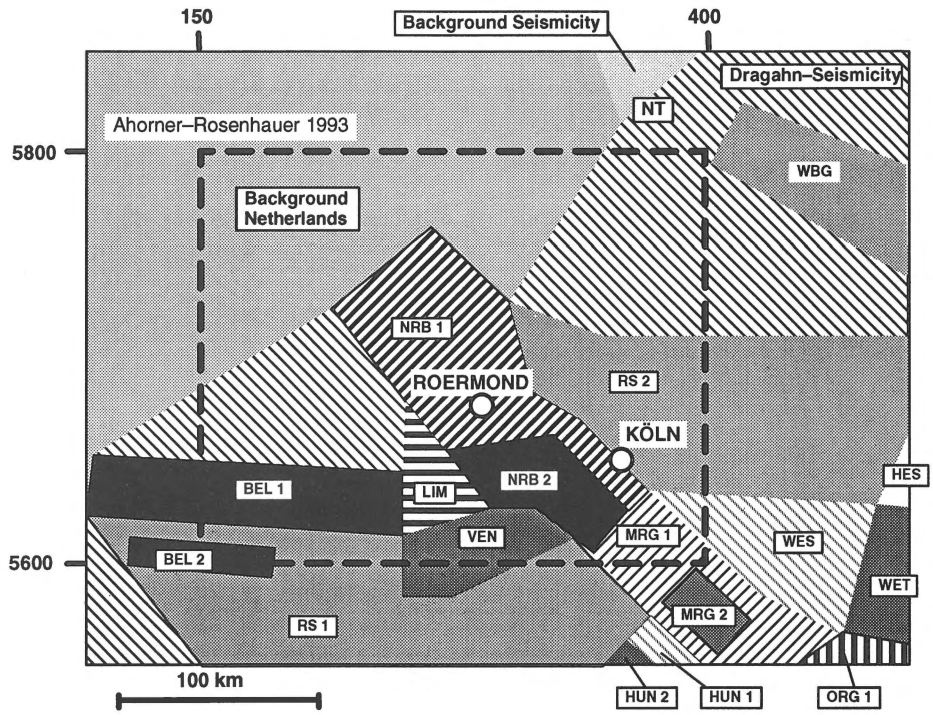

Fig. 3. Seismic zones near Roermond. Area for recomputation of seismic hazard bordered by broken lines. Coordinates UTM Zone 32U (km).

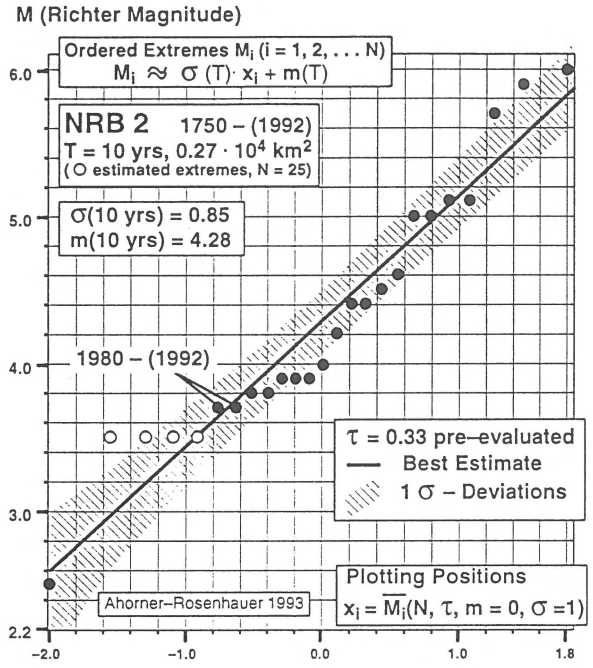

Fig. 4. 10-years' magnitude extremes for the seismic zone NRB 2 of the Lower Rhine Embayment, plotted according to the generalized Gumbel distribution. m (10 yrs) and σ (10 yrs) are taken from the plot, whereas the value of τ is required for its construction.

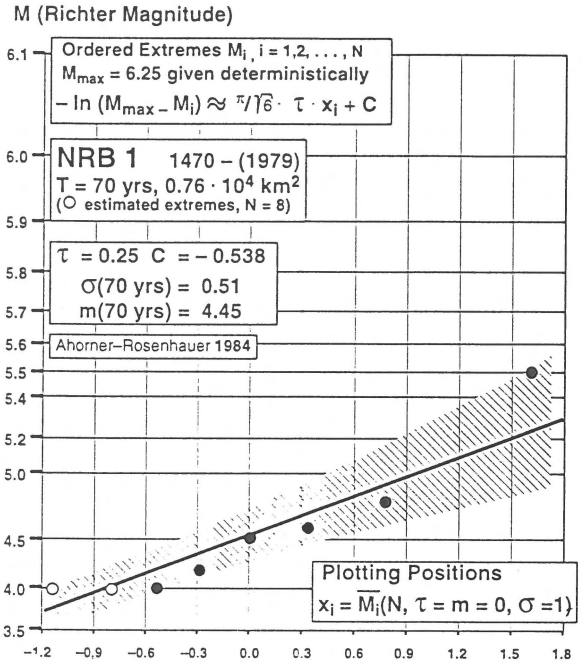

Fig. 5. 70-years' magnitude extremes up to 1979 for the seismic zone NRB 1 of the Lower Rhine Embayment, plotted according to the generalized Gumbel distribution. τ and C are taken from the plot, whereas the value of M_{max} is required for its construction.

m = 0 and σ = 1. These x_i are easily computed as mean values by a corresponding Monte-Carlo simulation, together with their standard deviations, resulting in hatched confidence ranges (Fig. 4).

The result is a plot illustrating the expected deviations of the extremes from the best estimate, giving an impression of the quality (or the inadequacies) achieved by the generalized Gumbel distribution. Estimated extremes (open circles in Fig. 4) fill in the blanks in 10-year intervals of the total period 1750–1992. They are assumed as largest events which plausibly might have been left unreported. Their exact values are unimportant, since the final results are based on as many sets of extremes as possible and are not significantly influenced by errors in the estimated extremes. Figure 4 shows just one of a total of nine data sets evaluated for NRB 2.

The Roermond earthquake occurred in NRB 1 and not in NRB 2. However, it is obvious from Fig. 4 that an event like the Roermond earthquake would also fit well into the seismicity of NRB 2, and it is equally evident that the additional data 1980–1992 does not lead to significant changes of the former evaluation.

Figures 5 and 6 compare two data sets with T = 70 years, one before and one after the Roermond earthquake, for the seimic zone NRB 1. An alternative straight line plot has to be applied here because N = 8, the total number of extremes including two estimated values, is insufficient for an independent statistical determination of the curvature parameter τ due to the inherent estimation uncertainties. This holds of course also for statistical estimates of M_{max}. $M_{max} = 6^1/_4$ was assumed deterministically before the Roermond earthquake, though $M_{max} = 6^1/_2$ seems to be more appropriate now, giving a better agreement of the results of the revised six data sets evaluated for NRB 1.

Figures 5 and 6 allow an unbiased dependent determination of τ, i.e. for a given M_{max}. This is due to the following exact relations between mean values, where i = 1 refers to the lowest, i = 2 to the second etc. value of N ordered extremes $M_1 \leqslant M_2 \leqslant \ldots \leqslant M_N$:

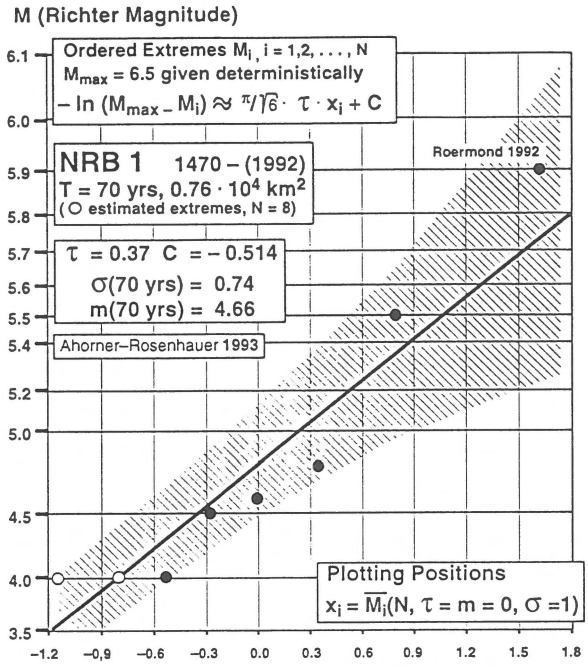

Fig. 6. 70-years' magnitude extremes including the Roermond 1992 earthquake for the seismic zone NRB 1 of the Lower Rhine Embayment, plotted according to the generalized Gumbel distribution. τ and C are taken from the plot, whereas the value of M_{max} is required for its construction.

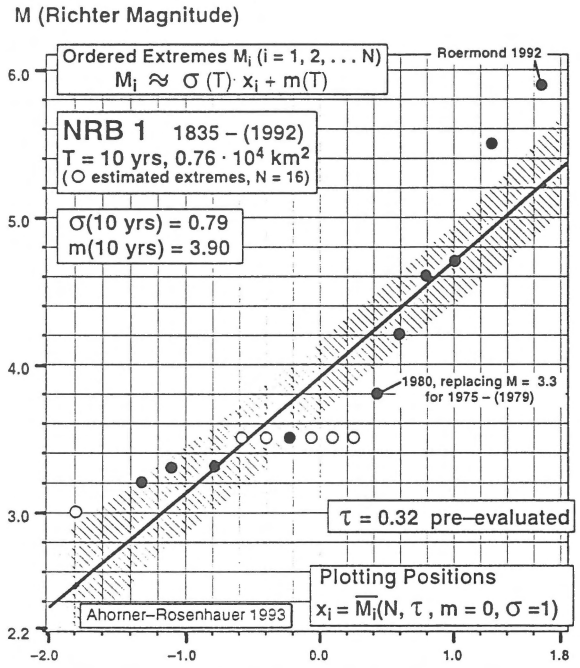

Fig. 7. 10-years' magnitude extremes for the seismic zone NRB 1 of the Lower Rhine Embayment, plotted according to the generalized Gumbel distribution. m (10 yrs) and σ (10 yrs) are taken from the plot, whereas the value of τ is required for its construction.

$$\overline{-\ln\left(f_1 - f_2 \frac{M_i - m(T)}{\sigma(T)}\right)^{1/\tau}} = \frac{\pi}{\sqrt{6}} \cdot \overline{M_i}(\tau = 0, m = 0, \sigma = 1) + E = \frac{\pi}{\sqrt{6}} \cdot x_i + E \qquad (3)$$

where E = 1.28255 (Euler's number).

Insertion of M_{max} from Eq. 1 yields the approximately linear dependence of the plotted 'observed' quantity – ln (M_{max}–M_i) upon the new x_i. These plotted quantities are not quite identical in Figs 5 and 6 because of the different values of M_{max}. The plotting positions x_i and their variances were again determined by a corresponding Monte-Carlo simulation, now for the special Gumbel distribution ($\tau = 0$) with m = 0 and σ = 1. A biased estimate of σ(T), which is only used for comparison, is obtained from inversion of

$$C = C(\sigma(T), \tau) = E + \ln(f_2/\sigma(T)) \qquad (4)$$

The change before and after the Roermond earthquake seems substantial when comparing Figs 5 and 6, but is less dramatic when including other data sets for NRB 1. This is illustrated by a second evaluation for NRB 1 in Fig. 7. As mentioned above it is an important part of the method to set up and evaluate as many nearly complete sets of extremes as possible for different T and several total periods.

Figure 8 shows the final frequency–magnitude results $\lambda(> M)$ (bold lines in Fig. 8) based on all evaluated data sets. The new evaluation confirms the former frequency–magnitude relation for NRB 2, which is the region of the strongest seismicity (uppermost curve in Fig. 8). The comparison of the new result using $M_{max} = 6^1/_2$ with that for data up to 1979 (dotted line in Fig. 8) exhibits a considerable change for NRB 1 due to the Roermond earthquake. The reason is not the increased value of M_{max}. Replacing $M_{max} = 6^1/_4$ for NRB 1 in favour of $M_{max} = 6^1/_2$ after the Roermond earthquake is seen to be of minor influence in the range of magnitudes M < 6 (compare broken line in Fig. 8).

The seismicity of 'Background Netherlands' (lowest curve in Fig. 8) is given as an example of the conservative quantitative treatment of extremely low seismicity. It is based on the information compiled in

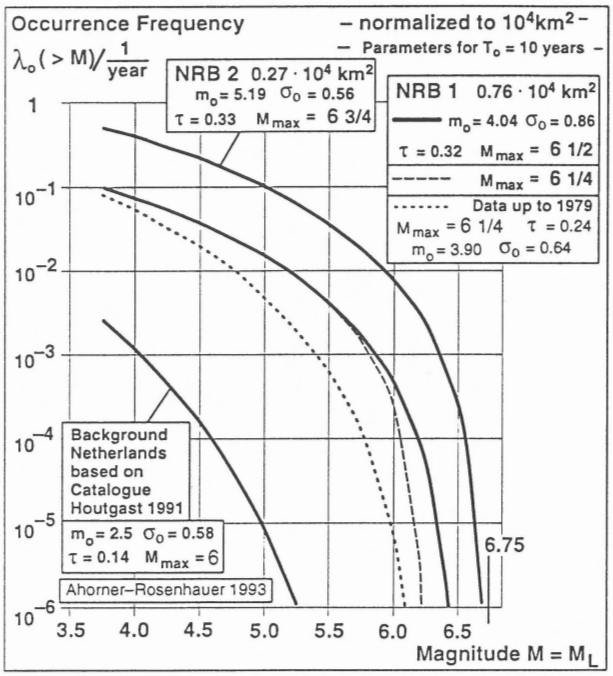

Fig. 8. Frequency–magnitude curves for the seismic zones NRB 1 and NRB 2 of the Lower Rhine Embayment and Background Netherlands according to the generalized Gumbel distribution. All curves are given for an area of 10^4 km^2 in order to allow comparison.

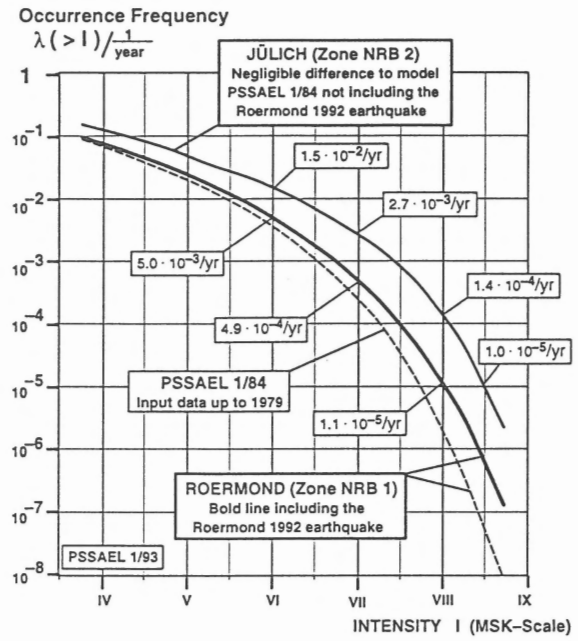

Fig. 9. Most probable epicentral distances and magnitudes for different site intensities at Roermond, Lower Rhine Embayment. The significance of the near environment (seismic zone NRB 1) is stronger for intensities > VI–VII after inclusion of the Roermond 1992 earthquake.

Houtgast (1991). The interpretation of this curve is that M > 6 is excluded (assumption of $M_{max} = 6$), and that the strongest event expected in any 10 years in 10^4 km^2 of this region is between magnitudes M = 1.9 (= $m_0 - \sigma_0$) and M = 3.1 (= $m_0 + \sigma_0$).

Hazard results and conclusions

The site intensity I(M, R) is computed for each simulated earthquake from its magnitude M and its hypocentral distance R (in km) by an individual law. This accounts for the significant scattering of the intensity attenuation and the intensity–magnitude correlation. These laws are obtained from the following equation for I(R, M) given with the parameters' notation of the code PSSAEL:

$$I(M,R) = 1.5 \cdot M - BM - AKH \cdot \log(R/10) - AKOF \cdot (R - 10) \quad (5)$$

where (AKOF = 0 for R < 10).
BM = 1.0 ± 0.6, AKH = 3.0, and AKOF = 0.003 were found in Ahorner (1983) for earthquakes in the

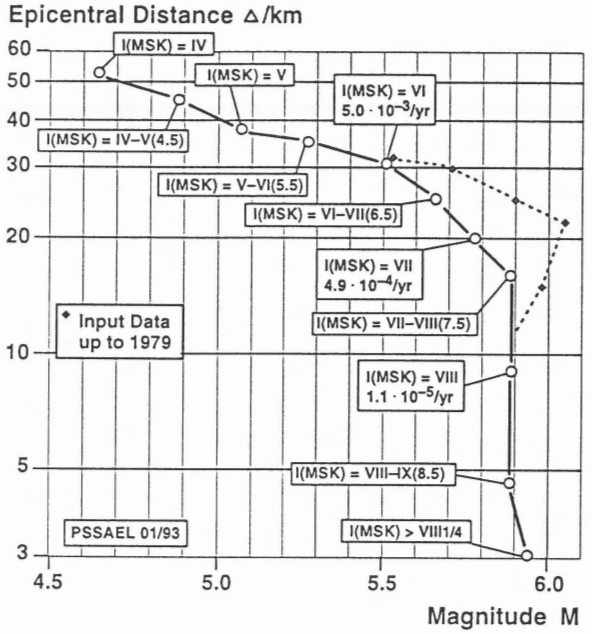

Fig. 10. Frequency–intensity curves for two sites in the seismic zones NRB 1 and NRB 2 of the Lower Rhine Embayment before (broken line) and after the Roermond 1992 earthquake.

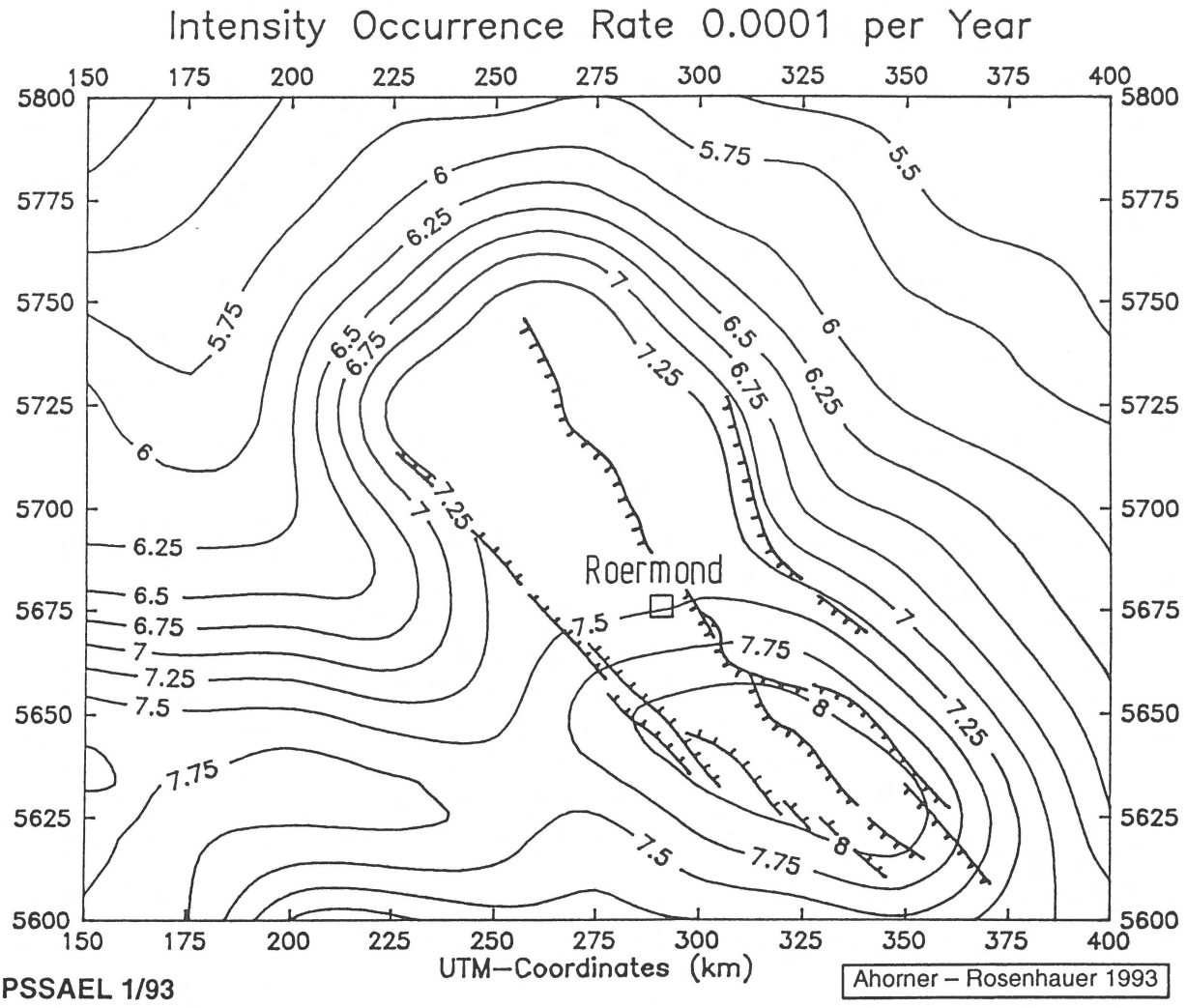

Fig. 11. Probabilistic earthquake intensity (MSK) isolines for the Lower Rhine Embayment; rate of occurrence $\lambda(> I) = 10^{-4}$/year. Lines with barbs (on downthrown side) denote active faults.

Rhine area. The parameter BM is simulated with a uniform distribution between 0.4 and 1.6. The probabilistic models of the other parameters are based on the same evaluation. For AKH a uniform distribution between 2.5 and 3.0 is chosen with 50% probability, and between 3.0 and 4.0 also with 50% probability. Logarithmic uniform distributions are applied for AKOF between 0.001 and 0.003 as well as 0.003 and 0.01 with a 50% probability in each range.

Two special sites are considered in order to study the effect of the Roermond earthquake on the seismicity risk assessment of the Lower Rhine Embayment: 1) Juelich centered in the more active seismic zone NRB 2, and 2) Roermond in the seismic zone NRB 1 in which the Roermond 1992 earthquake occurred.

The code PSSAEL produces extensive artificial earthquake catalogues by Monte-Carlo simulation of the seismicity model, i.e. it generates a collection of what might happen in a future time period by considering numerous independent repetitions of it. Specific earthquake libraries are created, selecting those events that produce an intensity in the interval I = IV $\pm$ 1/4, I = 4.5 $\pm$ 1/4 and so on at the site under investigation. These libraries of some hundred earthquakes each make it possible to obtain the most probable source parameters (mean values, Fig. 9) and corresponding standard deviations (not given here) of the earthquakes causing a certain future site intensity.

A comparison with older input data shows that possible earthquakes in NRB 2 (epicentral distance $\Delta >$

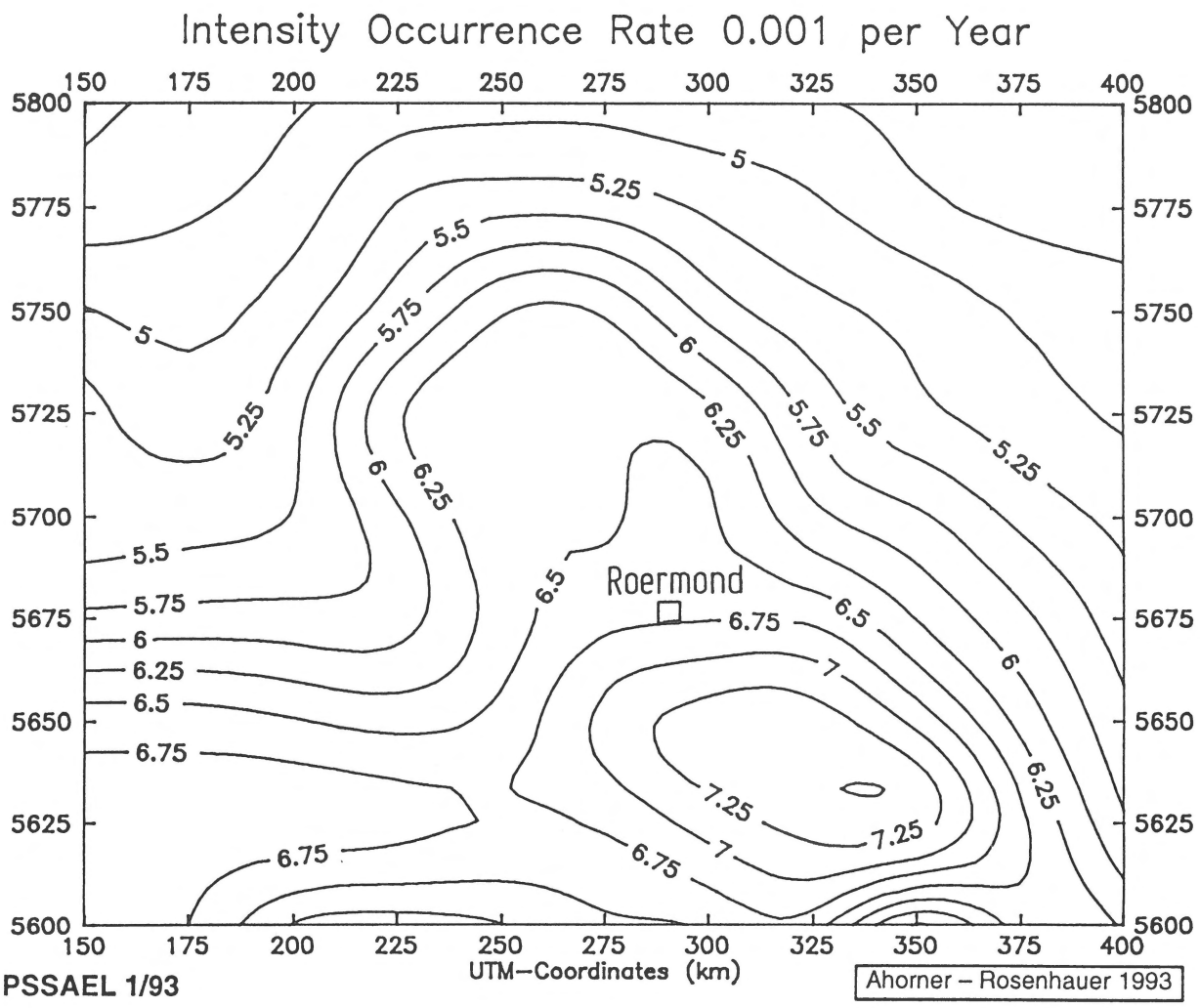

Fig. 12. Probabilistic earthquake intensity (MSK) isolines for the Lower Rhine Embayment; rate of occurrence $\lambda(> I) = 10^{-3}$/year.

15 km) loose their influence at site intensities between I = VI and about I = VIII for Roermond. These intensities are now caused by events smaller and significantly closer to the site because of the higher seismicity assessed for NRB 1 after the Roermond earthquake (Fig. 8). The conclusion, well known from many other site analyses, is that the occurrence of the smaller intensities is caused predominantly by events at larger epicentral distances, $\triangle > 30$ km for I < VI in this case (Fig. 9), and that the hazard is dominated by events significantly smaller than M_{max}. $M < 5.9 << M_{max} = 6^1/_2$ is found for site intensities up to I(MSK) > VIII$^1/_4$ at Roermond. This illustrates the, generally found, small sensitivity with respect to M_{max} and indicates the minor importance of the choice of $M_{max} = 6^1/_2$ for NRB 1 after the Roermond earthquake instead of $M_{max} = 6^1/_4$ before. The essential change is therefore expected from the considerable increase (about a factor of almost 10 between magnitudes M = 5.5 and M = 6) of the magnitude occurrence frequency $\lambda(> M)$ now derived for NRB 1 (Fig. 8).

The probabilities of the single intensity intervals I = IV $\pm$ 1/4 and so on are easily obtained from the number of repetitions (see above) required in generating the corresponding earthquake libraries. Figure 10 presents the new frequency–intensity relation $\lambda(> I)$ for Roermond (middle curve in Fig. 10). It is numerically identical with a result of De Crook (1993), which was achieved by a different approach. A computation with $\lambda(> M)$ for the new extremes but old upper bound

M_{max} = $6^1/_4$ (broken line in Fig. 8) confirmed the negligible differences as expected.

The old result 'PSSAEL 1/84' (broken line in Fig. 10) is given for comparison. The magnitude difference at equal probability levels of up to $\triangle M = 0.5$ between old and new frequency–magnitude curves $\lambda(> M)$ in Fig. 8 might perhaps suggest a corresponding shift between the Roermond frequency–intensity curves $\lambda(> I)$. The influence of the more distant and unchanged regions of higher seismicity (especially NRB 2) cannot, however, be neglected. Thus, considering for instance the level of 10^{-5}/year, a shift of the curve of only 1/4 intensity degree is found in Fig. 10, I = 8.75 versus 8.5. The result for Juelich situated in seismic zone NRB 2 (uppermost curve in Fig. 10) was recalculated resulting in insignificant changes and confirming, on the other hand, that the influence of NRB 1 is negligible for that site.

The frequencies $\lambda(> I)$ of eleven intensities between IV and IX were recomputed for a grid of 99 sites (grid width 25 km) as a basis of redrawn hazard maps for the Lower Rhine Embayment. The intensities with occurrence frequencies 10^{-4}/year and 10^{-3}/year were determined by interpolation from these results for each of the 99 sites and then evaluated by drawing iso-intensity lines. The resulting maps are Fig. 11 for the occurrence frequency level of 10^{-4}/year, including the main fault lines for better orientation, and Fig. 12 for the level of 10^{-3}/year. The higher frequency is associated with smaller intensities, which are most probably caused by earthquakes at larger distances (Fig. 9). This is the reason why the original seismic zones are less clearly visible in Fig. 12.

The occurrence of a single extraordinary event like the Roermond 1992 earthquake may suggest a significantly increased and hitherto underestimated seismic hazard at first sight. It may even induce, as has been shown, an increase of the most uncertain but less important input parameters of a probabilistic hazard assessment, the upper magnitude bounds, M_{max}. A repetition at the same place is, on the other hand, not likely, and only moderate changes of the probabilistic results have been found.

The Roermond 1992 earthquake gave rise to distinct corrections of the assessed regional magnitude occurrence frequencies $\lambda(> M)$. The final decisive conclusion is, however, that the available methods of probabilistic seismic hazard analysis cope with the problem and are providing extremely stable results.

References

Ahorner, L. 1983 Seismicity and neotectonic structural activity of the Rhine Graben system in Central Europe. In: A.R. Ritsema & A. Gürpinar (eds.): Seismicity and Seismic Risk in the Offshore North Sea Area. – D. Reidel Publ. Co., Dordrecht: 101–111

Ahorner, L. & W. Rosenhauer 1975 Probability distribution of earthquake accelerations with applications to sites in the northern Rhine area, Central Europe – J. Geophys. 41: 581–594

Ahorner, L. & W. Rosenhauer 1986 Regionale Erdbebengefährdung. In: Realistische Seismische Lastannahmen für Bauwerke. Abschlußbericht an das Institut für Bautechnik Berlin – König und Heunisch, Beratende Ingenieure, Frankfurt/Erdbebenstation Bensberg der Universität Köln / Institut für Geophysik der Universität Stuttgart: 334 pp.

Ahorner, L. & W. Rosenhauer 1993 Seismische Risikoanalyse. In: Naturkatastrophen und Katastrophenvorbeugung. Bericht zur Int. Decade Natural Disaster Reduction, Deutsche Forschungsgemeinschaft – VCH-Verlag, Weinheim: 177–190 pp

Burton, P.W. 1979 Seismic risk in southern Europe through India examined using Gumbel's third distribution of extreme values – Geophys. J.R. Astr. Soc. 59: 249–280

De Crook, Th. 1993 Earthquake hazard for Roermond, the Netherlands – Geol. Mijnbouw, this issue

Hosser, D. & R. Maurer 1986 Statistische Freifeldspektren. In: Realistische Seismische Lastannahmen für Bauwerke. Abschlußbericht an das Institut für Bautechnik Berlin – König und Heunisch, Beratende Ingenieure, Frankfurt / Erdbebenstation Bensberg der Universität Köln / Institut für Geophysik der Universität Stuttgart: 334 pp

Hosser, D., H. Klein, L. Ahorner, W. Rosenhauer, H. Berckhemer, J. Kopera, G. Schneider, Th. Kunze, G. Waas, H. Werkle & W. Weber 1983 Realistische Seismische Lastannahmen für bauliche Anlagen mit erhöhtem Sekundärrisiko. Abschlußbericht im Auftrag des Institut für Bautechnik, Berlin – König und Heunisch Beratende Ingenieure, Frankfurt: 236 pp

Houtgast, G. 1991 Catalogus aardbevingen in Nederland – Kon. Ned. Meteor. Inst. (KNMI), publ. 179: 166 pp

Rosenhauer, W. 1983 Methodological aspects encountered in the Lower Rhine area seismic hazard analysis. In: A.R. Ritsema & A. Gürpinar (eds.): Seismicity and Seismic Risk in the Offshore North Sea Area – D. Reidel Publ. Co., Dordrecht: 385–396

Rosenhauer, W. 1984 Seismizitätsanalyse und probabilistische Erdbebengefährdungskarten für ein die Bundesrepublik imfassendes Gebiet. Abschlußbericht im Auftrag der Siemens Kraft Werk Union – Interatom-Bericht 68.08753.3: 45 pp

Rosenhauer, W. & L. Ahorner 1991 Spezielle Untersuchungen zür Magnituden-Häufigkeits-Relation für die Seismische Risikoanalyse. In: P. Knoll & D. Werner (eds.): Erdbeben – Ingenieurwesen – Vortragsband des Koloquiums 'Erdbebeningenieurwesen und Baudynamik' 9–11 Januar 1991 – Zentralinstitut für Physik der Erde, Potsdam: 155–172 pp